DOI 10.1007/s10778-017-0837-z
International Applied Mechanics, Vol. 53, No. 5, September, 2017

PROPAGATION OF AXISYMMETRIC ELECTROELASTIC WAVES IN A HOLLOW LAYERED CYLINDER UNDER MECHANICAL EXCITATION

A. Ya. Grigorenko[1] and I. A. Loza[2]

The problem on propagation of axisymmetric electroelastic waves in a hollow layered cylinder made of metallic and radially polarized piezoceramic layers is solved. The lateral surfaces of the cylinder are free of electrodes. The outside surface is free of mechanical loads, while the inside one undergoes harmonically varying pressure Pe. The problem was solved with a numerical-analytical method. By representing the components of the stress tensor, displacement vectors, electric-flux density, and electrostatic potential by traveling waves, the original electroelastic problem in partial derivatives is reduced to an inhomogeneous boundary-value problem for ordinary differential equations. To solve the problem, the stable numerical discrete-orthogonalization method is used. The results of the kinematic analysis of the layered cylinder both with metallic and piezoceramic (PZT 4) layers are presented. The numerical results are analyzed.

Keywords: kinematic analysis of electroelastic waves, layered hollow cylinders, discrete orthogonalization

Introduction. The problem on propagation of elastic waves in circular cylinders is addressed in a great many studies reviewed in [1, 2, 11, 12, etc.]. The coupled fields strongly complicate the study [3, 4, 6, 7, et. al.]. The solution for a piezoceramic cylinder (only in the case of axial polarization for longitudinal axisymmetric waves as well as in the case of circumferential polarization for torsional waves) can be represented in terms of special functions. The allowance for the material heterogeneity makes the problem more complicated, whereas heterogeneous piezoelectric materials (bimorphs) are employed in many devices. The interface between two media requires the conditions of joining the unknown functions at it to be satisfied. The results of appropriate studies are presented in [5, 8–10, 13, etc.].

In what follows, we will consider an axisymmetric problem on propagation of forced acoustoelectric waves in a layered hollow cylinder with piezoceramic and metallic layers. To solve the problem, we will employ an effective numerical-analytical approach. Using it, the kinematic analysis of the acoustoelectric waves propagating along the cylinder axis will be carried out. We will also study how the heterogeneity influences the kinematic characteristics of propagating waves.

1. Problem Statement. Basic Equations for Hollow Cylinders. The axisymmetric longitudinal equations of motion of the *j*th layer as well as the equations of electrostatics and kinematic relations in the cylindrical coordinate system (r, θ, z) take the following form, respectively [8]:

$$\frac{\partial \sigma_{rr}^i}{\partial r} + \frac{\sigma_{rr}^i - \sigma_{\theta\theta}^i}{r} + \frac{\partial \sigma_{rz}^i}{\partial z} = \rho^i \frac{\partial^2 u_r^i}{\partial t^2},$$

$$\frac{\partial \sigma_{rz}^i}{\partial r} + \frac{\sigma_{rz}^i}{r} + \frac{\partial \sigma_{zz}^i}{\partial z} = \rho^i \frac{\partial^2 u_z^i}{\partial t^2}. \qquad (1)$$

[1]S. P. Timoshenko Institute of Mechanics, National Academy of Sciences of Ukraine, 3 Nesterova St., Kyiv, Ukraine 03057, e-mail: ayagrigorenko@yandex.ru. [2]National Transport University, 1 Omelyanovicha-Pavlenko St., Kyiv, Ukraine 01010; e-mail: dukeigor@mail.ru. Translated from Prikladnaya Mekhanika, Vol. 53, No. 5, pp. 94–100, September–October, 2017. Original article submitted July 4, 2016.

$$\frac{\partial D_r^i}{\partial r}+\frac{D_r^i}{r}+\frac{\partial D_z^i}{\partial z}=0, \qquad E_r^i=-\frac{\partial \varphi^i}{\partial r}, \qquad E_z^i=-\frac{\partial \varphi^i}{\partial z}. \tag{2}$$

$$\varepsilon_{rr}^i=\frac{\partial u_r^i}{\partial r}, \qquad \varepsilon_{\theta\theta}^i=\frac{u_r^i}{r}, \qquad \varepsilon_{zz}^i=\frac{\partial u_z^i}{\partial z}, \qquad \varepsilon_{rz}^i=\frac{1}{2}\left(\frac{\partial u_r^i}{\partial z}+\frac{\partial u_z^i}{\partial r}\right). \tag{3}$$

Here σ_{ij}^i are the components of the stress tensor, ρ^i is the density of the material, ω is the circular frequency, u_i^i are the components of the displacement vector, D_i^i are the components of the electric-flux density, E_i^i are the components of electric-field strength, φ^i is electrostatic potential, ε_{ij}^i are the components of the strain tensor.

Let us represent the constitutive equations for the *j*th radially polarized piezoceramic layer as follows:

$$\sigma_{rr}^i=c_{33}^i\varepsilon_{rr}^i+c_{13}^i\varepsilon_{\theta\theta}^i+c_{13}^i\varepsilon_{zz}^i-e_{33}^iE_r^i,$$

$$\sigma_{\theta\theta}^i=c_{13}^i\varepsilon_{rr}^i+c_{11}^i\varepsilon_{\theta\theta}+c_{12}^i\varepsilon_{zz}-e_{31}^iE_r^i,$$

$$\sigma_{zz}^i=c_{13}^i\varepsilon_{rr}^i+c_{12}^i\varepsilon_{\theta\theta}+c_{11}^i\varepsilon_{zz}^i-e_{31}^iE_r^i, \qquad \sigma_{rz}^i=2c_{55}^i\varepsilon_{rz}^i-e_{51}^iE_z,$$

$$D_r^i=e_{33}^i\varepsilon_{rr}^i+e_{31}^i\varepsilon_{\theta\theta}^i+e_{31}^i\varepsilon_{zz}^i+\varepsilon_{33}^iE_r^i, \qquad D_z^i=2e_{51}^i\varepsilon_{rz}^i+\varepsilon_{33}^iE_z^i, \tag{4}$$

where c_{ij}^i are the components of the tensor of elastic moduli, e_{ij}^i are the components of the tensor of piezomoduli, ε_{ij}^i are the components of the tensor of dielectric permittivity.

The constitutive relations for the *i*th metallic layer are:

$$\sigma_{rr}^i=\frac{(1-\nu^i)E^i}{(1+\nu^i)(1-2\nu^i)}\varepsilon_{rr}^i+\frac{\nu^iE^i}{(1+\nu^i)(1-2\nu^i)}\varepsilon_{\theta\theta}^i+\frac{\nu^iE^i}{(1+\nu^i)(1-2\nu^i)}\varepsilon_{zz}^i,$$

$$\sigma_{\theta\theta}^i=\frac{\nu^iE^i}{(1+\nu^i)(1-2\nu^i)}\varepsilon_{rr}^i+\frac{(1-\nu^i)E^i}{(1+\nu^i)(1-2\nu^i)}\varepsilon_{\theta\theta}+\frac{\nu^iE^i}{(1+\nu^i)(1-2\nu^i)}\varepsilon_{zz},$$

$$\sigma_{zz}^i=\frac{\nu^iE^i}{(1+\nu^i)(1-2\nu^i)}\varepsilon_{rr}^i+\frac{\nu^iE^i}{(1+\nu^i)(1-2\nu^i)}\varepsilon_{\theta\theta}+\frac{(1-\nu^i)E^i}{(1+\nu^i)(1-2\nu^i)}\varepsilon_{zz}^i,$$

$$\sigma_{rz}^i=2\frac{E^i}{2(1+\nu^i)}\varepsilon_{rz}^i, \tag{5}$$

where ν is Poisson's ratio, E is the Young modulus (hereinafter the index i will be omitted).

We prescribe the following boundary conditions on the lateral surfaces of the cylinder (for $r=R_0\pm h$):

– the surfaces are not covered by electrodes: $D_r|_{r=R_0\pm h}=0$;

– the outside surface of the cylinder is free of external forces: $\sigma_{rr}|_{r=R_0+h}=\sigma_{rz}|_{r=R_0+h}=0$;

– the inside surface is under harmonically varying pressure: $\sigma_{rr}|_{r=R_0-h}=Pe^{i(kz-\omega t)}$, $\sigma_{rz}|_{r=R_0-h}=0$.

Here R_0 is the radius of the mid-surface of the cylinder; h is its half-thickness.

The vector of unknowns in mixed form is

$$R=\{\sigma_{rr},\sigma_{rz},\varphi,u_r,u_z,D_r\}^T. \tag{6}$$

Resolving system (1)–(4) for R and performing some transformations, we get

$$\frac{\partial \sigma_{rr}}{\partial r} = \frac{1}{r}\left(\frac{\Delta_2}{\Delta} - 1\right)\sigma_{rr} - \frac{\partial \sigma_{rz}}{\partial z} - \left(\frac{\Delta_3}{r^2\Delta} - \rho\frac{\partial^2}{\partial t^2}\right)u_r - \frac{\Delta_4}{r\Delta}\frac{\partial u_z}{\partial z} - \frac{\Delta_1}{r\Delta}D_r,$$

$$\frac{\partial \sigma_{rz}}{\partial r} = \frac{\Delta_2}{\Delta}\frac{\partial \sigma_{rr}}{\partial z} - \frac{1}{r}\sigma_{rz} + \frac{\Delta_5}{r\Delta}\frac{\partial u_r}{\partial z} - \left(\frac{\Delta_6}{\Delta}\frac{\partial^2}{\partial z^2} - \rho\frac{\partial^2}{\partial t^2}\right)u_z - \frac{\Delta_1}{\Delta}\frac{\partial D_r}{\partial z},$$

$$\frac{\partial \varphi}{\partial r} = \frac{e_{33}}{\Delta}\sigma_{rr} + \frac{\Delta_1}{r\Delta}u_r + \frac{\Delta_1}{\Delta}\frac{\partial u_z}{\partial z} - \frac{c_{33}}{\Delta}D_r,$$

$$\frac{\partial u_r}{\partial r} = \frac{\varepsilon_{33}}{\Delta}\sigma_{rr} - \frac{\Delta_2}{r\Delta}u_r - \frac{\Delta_2}{\Delta}\frac{\partial u_z}{\partial z} + \frac{e_{33}}{\Delta}D_r,$$

$$\frac{\partial u_z}{\partial r} = \frac{1}{c_{55}}\sigma_{rz} - \frac{\partial u_r}{\partial z} - \frac{e_{51}}{rc_{55}}\frac{\partial \varphi}{\partial z},$$

$$\frac{\partial D_r}{\partial r} = -\frac{e_{51}}{c_{55}}\frac{\partial \sigma_{rz}}{\partial z} + \frac{\Delta_7}{c_{55}}\frac{\partial^2 \varphi}{\partial z^2} - \frac{1}{r}D_r, \tag{7}$$

where

$$\Delta = c_{33}\varepsilon_{33} + e_{33}^2, \quad \Delta_1 = c_{33}e_{13} - c_{13}e_{33}, \quad \Delta_2 = c_{13}\varepsilon_{33} + e_{13}e_{33},$$

$$\Delta_3 = (c_{13} - c_{33})\Delta_2 + (e_{33} - e_{13})\Delta_1 + (c_{13} - c_{11})\Delta,$$

$$\Delta_4 = (c_{13} - c_{33})\Delta_2 + (e_{33} - e_{13})\Delta_1 + (c_{13} - c_{12})\Delta,$$

$$\Delta_5 = c_{12}\Delta + e_{13}\Delta_1 - c_{13}\Delta_2, \quad \Delta_6 = c_{11}\Delta + e_{13}\Delta_1 - c_{13}\Delta_2, \quad \Delta_7 = c_{55}\varepsilon_{11} + e_{15}^2.$$

2. Technique of Solving Axisymmetric Boundary-Value Problems. Let us represent the solution in the form of waves traveling in the axial direction:

$$\sigma_{rr}(r,z,t) = \lambda\sigma_{rr}(r)e^{i(kz-\omega t)}, \quad \sigma_{rz}(r,z,t) = i\lambda\sigma_{rz}(r)e^{i(kz-\omega t)},$$

$$\varphi(r,z,t) = h\sqrt{\frac{\lambda}{\varepsilon_0}}\varphi(r)e^{i(kz-\omega t)}, \quad u_r(r,z,t) = hu_r(r)e^{i(kz-\omega t)},$$

$$u_z(r,z,t) = hu_z(r)e^{i(kz-\omega t)}, \quad D_r(r,z,t) = \sqrt{\varepsilon_0\lambda}D_r(r)e^{i(kz-\omega t)}. \tag{8}$$

With (8), the original two-dimensional electroelastic problem in partial derivatives (7) can be reduced to a boundary-value problem for ordinary differential equations [8]:

$$\frac{d\mathbf{R}}{dx} = A(x,\Omega)\mathbf{R}, \tag{9}$$

with boundary conditions

$$\mathbf{B}_1\mathbf{R}(-1) = \mathbf{C}_1, \quad \mathbf{B}_2\mathbf{R}(1) = \mathbf{C}_2, \tag{10}$$

where $\mathbf{C}_1^T = \{0, 0, 0, 0, 0, 0\}$ and $\mathbf{C}_2^T = \{P, 0, 0, 0, 0, 0\}$. Here

$$\Omega = \omega h\sqrt{\frac{\rho_0}{\lambda}}, \quad \tilde{c}_{ij} = \frac{c_{ij}}{\lambda}, \quad \tilde{e}_{ij} = \frac{e_{ij}}{\sqrt{\varepsilon_0\lambda}}, \quad \tilde{\varepsilon}_{ij} = \frac{\varepsilon_{ij}}{\varepsilon_0}, \quad x = \frac{r - R_0}{h},$$

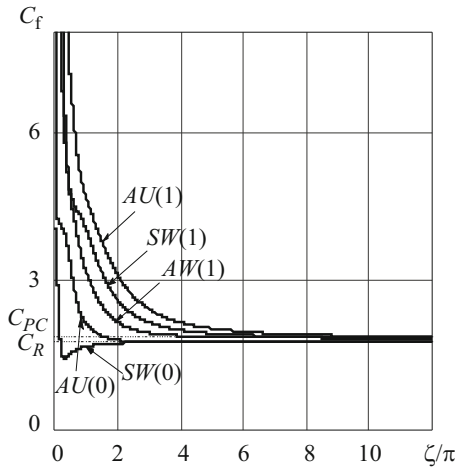

Fig. 1

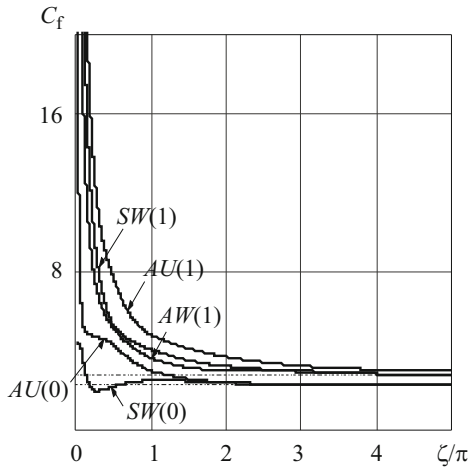

Fig. 2

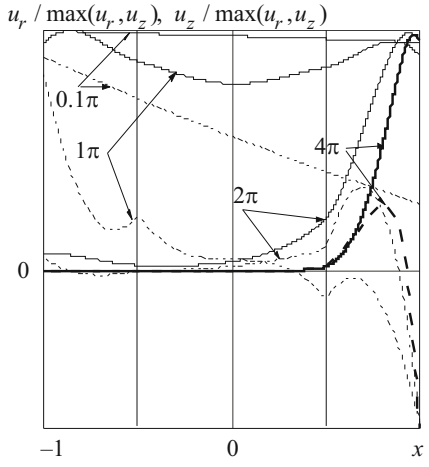

Fig. 3

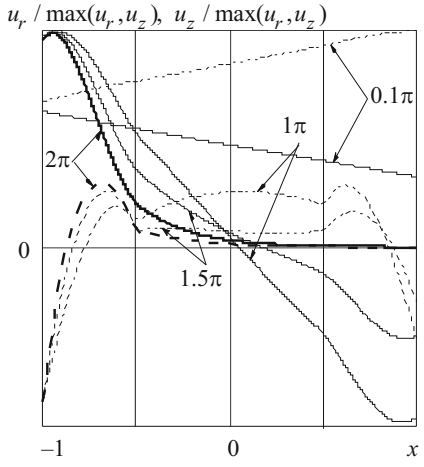

Fig. 4

ε_0 is the dielectric permittivity of vacuum; $\lambda = 10^{10}$ N/m^2, $\rho_0 = 1$ kg/m^3.

To solve problem (9), (10), we use the stable discrete-orthogonalization method in combination with the step-by-step search method.

3. Analysis of Numerical Results. Let us consider the results of numerical analysis of problem (9), (10) for a three-layer cylinder whose face layers are made of PZT ceramic while the core layer is made of steel with $\nu = 0.28$ and $E = 21$; curvature parameter $\varepsilon = 0.25$. The thicknesses of the face and core layers are h and $2h$, respectively.

Figure 1 shows the phase velocities for the first five waves in the case of a homogeneous cylinder made of PZT piezoceramic with lateral surfaces without electrodes. The notation is the same as in [6]. The notation $SW(0)$ means that the waves are represented ($k = 0$) as symmetric longitudinal oscillations (oscillations in expansion/compression wave), while $AU(0)$ as antisymmetric (flexural) radial oscillations. It follows from Fig. 1 that the first two branches $SW(0)$ and $AU(0)$ within a short-wave range tend to a similar velocity and propagate practically without dispersion. The kinematic analyses of these branches show that they represent Rayleigh-type waves. The other branches also tend to waves propagating without dispersion and are called Pochhammer–Chree waves, by analogy with Lamb waves for plates.

Figure 2 shows the phase velocities for the first five waves in the layered cylinder. As can be seen, the first two waves transform into a Rayleigh-type wave. The higher branches in the short-wave range pairwise converge, as can be seen for the $AW(1)$ and $SW(1)$ branches.

Let us analyze how the distribution of displacements varies in the layered cylinder across the thickness depending on the wave length. Figure 3 shows the distribution of the displacement amplitudes over the thickness $-1.0 \le h \le 1.0$ in the first wave

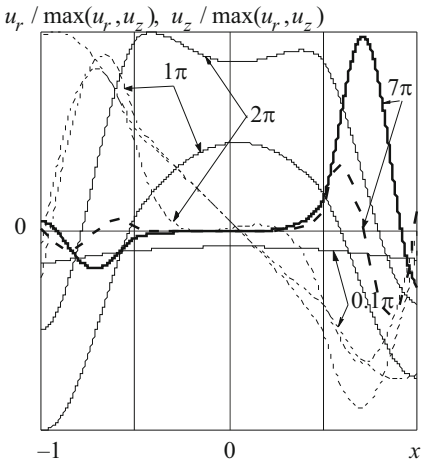

Fig. 5

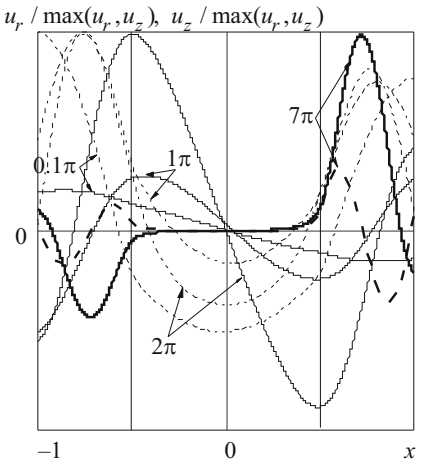

Fig. 6

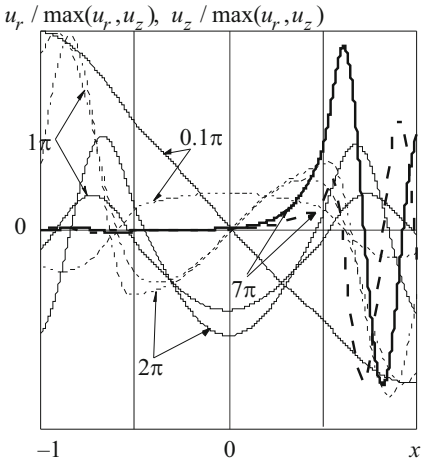

Fig. 7

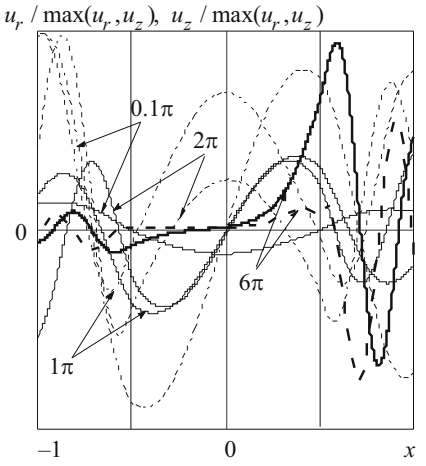

Fig. 8

$SW(0)$ for different values of the wave length. The solid line corresponds to the amplitudes of the radial displacements u_r, and the dashed line to the longitudinal displacements u_z. The distribution of the amplitudes of the displacements in the short-wave domain is shown by heavy lines. In the case of long waves, the displacement amplitudes are distributed nearly linearly. The displacement waves are concentrated with decreasing length near the outside lateral surface. In this case, the displacements are distributed as in Rayleigh waves.

Figure 4 shows the distribution of the displacement amplitudes across the thickness in the second wave $AU(0)$. Note that in the case of long waves, this distribution is linear. With decrease in the wave length, the displacements are concentrated on the inside lateral surface of the cylinder. Here the displacements are distributed as in Rayleigh waves.

Figure 5 shows the distribution of the displacement amplitudes across the thickness in the third wave $AW(1)$. As in the case of long waves, the displacement amplitudes are distributed across the thickness nonlinearly. With decrease in the wave length, the displacements are concentrated in the softer piezeceramic layers, whereas the steel layer remains undeformed. The displacements peak in the piezoceramic face layer.

Figure 6 shows the distribution of the displacement amplitudes across the thickness in the fourth wave $SW(1)$. As can be seen, with decrease in the wave length, not only the velocities of waves in both branches become similar but also the manner in which the displacements are distributed in them.

The situation is similar for the other two branches. In the short-wave domain, they approach each other and the displacement distribution across the thickness becomes similar. The distributions of displacement amplitudes across the thickness in the fifth wave $AU(1)$ and in the sixth wave $AW(2)$ are shown in Fig. 7 and 8. The displacements are concentrated in

the softer layer, whereas the steel layer remains undeformed. Despite the symmetry of the structure about the mid-surface, the displacements concentrate in the layer with lower curvature.

4. Conclusions. We have established the following. The first branch in the short-wave range, as in a cylinder made of a homogeneous material, tends to a Rayleigh-type wave propagating along the outside surface of the cylinder. The second wave tends to a Rayleigh-type wave propagating along the inside surface of the cylinder. For the higher branches, there are substantial differences in the distribution of displacement amplitudes. If the material is homogeneous, with decrease in the wave length, the displacement amplitudes distribute either symmetrically or antisymmetrically about the cylinder mid-surface. If the material is inhomogeneous, with decrease in the wave length, the dispersion branches approach each other pairwise and the distribution of displacement across the thickness becomes pairwise similar. The displacements concentrate in the softer piezoceramic layer with the lower curvature whereas the stiffer steel layer remains undeformed.

REFERENCES

1. V. T. Grinchenko and V. V. Meleshko, *Harmonic Vibrations and Waves in Elastic Bodies* [in Russian], Naukova Dumka, Kyiv (1981).
2. H. Kolsky, *Stress Waves in Solids*, Clarendon, Oxford (1953).
3. V. T. Grinchenko, A. F. Ulitko, and N. A. Shul'ga, *Electroelasticity*, Vol. 5 of the five-volume series *Mechanics of Coupled Fields in Structural Members* [in Russian], Naukova Dumka, Kyiv (1989).
4. W. P. Mason (ed.), *Physical Acoustics*, *Principles and Methods*, Vol. 1, *Part A: Methods and Devices*, Academic Press, New York–London (1964).
5. N. A. Shul'ga, "Propagation of harmonic waves in anisotropic piezoelectric cylinders, waveguides with complicated properties," in: Vol. 3 of the six-volume series *Advances in Mechanics* [in Russian], A.S.K., Kyiv (2007), pp. 651–680.
6. N. A. Shul'ga, A. Ya. Grigorenko, and I. A. Loza, "Axisymmetric electroelastic waves in a hollow piezoceramic cylinder," *Int. Appl. Mech.*, **20**, No. 1, 23–28 (1984).
7. M. C. Dokmeci, *A Dynamic Analysis of Piezoelectric Strained Elements*, Research Development and Standartization Group, New York (1992).
8. A. Ya. Grigorenko and I. A. Loza, "Axisymmetric waves in layered hollow cylinders with axially polarized piezoceramic layers," *Int. Appl. Mech.*, **47**, No. 6, 707–713 (2011).
9. A. Ya. Grigorenko and I. A. Loza, "Nonaxisymmetric waves in layered hollow cylinders with radially polarized piezoceramic layers," *Int. Appl. Mech.*, **49**, No. 6, 641–649 (2013).
10. A. Ya. Grigorenko and I. A. Loza, "Nonaxisymmetric waves in layered hollow cylinders with axially polarized piezoceramic layers," *Int. Appl. Mech.*, **50**, No. 2, 150–158 (2014).
11. A. N. Guz and F. G. Makhort, "The physical fundamentals of the ultrasonic nondestructive stress analysis of solids," *Int. Appl. Mech.*, **36**, No. 9, 1119–1149 (2000).
12. R. N. Thurston, "Elastic waves in rods and clad rods," *J. Acoust Soc. Am.*, **64**, No. 1, 1–37 (1978).
13. J. Wang and Z. Shi, "Models for designing radially polarized multilayer piezocelectric/elastic composite cylindrical transducers," *J. of Intelligent Material Systems and Structures*, **27**, No. 4, 500–511 (2016).